Progress In Electromagnetics Research, Vol. 111, 407–418, 2011

ACHIEVING LARGE EFFECTIVE APERTURE ANTENNA WITH SMALL VOLUME BASED ON COORDINATE TRANSFORMATION

D. Ye and S. Xi

Department of Information and Electronic Engineering
Zhejiang University, Hangzhou 310027, China

H. Chen

The Electromagnetics Academy at Zhejiang University
Zhejiang University, Hangzhou 310058, China

J. Huangfu and L. Ran

Department of Information and Electronic Engineering
Zhejiang University, Hangzhou 310027, China

Abstract—The size of an antenna should be relatively large in order to get high radiation directivity. However, in some applications, the antenna is restricted in small region, while high directivity is still required. In this paper, we propose the method of realizing antenna with large effective apertures using arbitrary shaped small PEC reflectors and small volumes of left-handed materials based on coordinate transformation. This design method is validated by the numerical simulations based on the Finite Element Method (FEM).

1. INTRODUCTION

Recently, the coordinate transformation method is introduced to the applications of metamaterials, such as invisibility cloaks [1–14], directive emission antenna [15, 16], waveguide bend devices [17–20]. Perfect invisibility spherical cloak for full waves was obtained through a proper coordinate transformation which compresses a spherical region into a concentric spherical shell, leaving the electromagnetic

Received 13 August 2010, Accepted 10 December 2010, Scheduled 17 December 2010
Corresponding author: Jiangtao Huangfu (huangfujt@zju.edu.cn).

wave detoured without interacting with any object inside the shell. Invisibility cloaks based on other techniques have also been proposed and extensively studied [21–23]. According to the transformation method, a type of cylindrical perfect lens which is achieved by rolling up a perfect slab lens in the virtual EM space was proposed [24]. In [2, 25], the perfect lenses and negative index material were shown to be results of multi-valued coordinate transformations. Based on this concept, cylindrical super-lenses with finite size, which is capable of magnification, were proposed [26]. Later, this concept was further developed to realize superscatterers, which are used to enlarge the scattering cross-section of a small object. In addition, the coordinate transformation method has also been applied to the design of high directivity antenna [27, 28] and manipulation of directivity of the antenna. The simulation results show that very directivity is achieved using this method. However, like conventional antenna including the new kinds of antenna based on metamaterials [29–35], the cross section of the antenna must be large enough in order to get the expected high directivity.

All the previous methods to achieve high directivity are deficient, which need large enough aperture of antenna. Different from those, we propose an exceptional technique to achieve antenna with large effective aperture to achieve high directivity but small cross sections, and a technique to achieve an antenna when the device is located at a distance away from the position where the effective antenna works. Small reflectors with arbitrary shapes can be used to achieve such antenna. For simplicity, we use small parabolic PEC reflector and semicircular PEC reflectors as examples, showing the design procedures. Through the FEM based numerical simulations, the design method is validated, and the enlarged effective apertures are observed.

2. TRANSFORMATION PROCEDURE FOR REALIZING LARGE APERTURE ANTENNA FROM SMALL REFLECTORS

Figures 1(a) and (b) show the transformation scheme to realize the proposed antenna. By applying the transformation function shown in Fig. 1(b), the region in the original space $0 < \rho < c$ is compressed into the space $0 < \rho' < a$ and a negative index region is created as a result of the transformation function in region $a < \rho' < b$. The small arbitrary reflector indicated by the function $\rho' = g(\phi')$ now has an image $\rho = G(\phi)$ in the region $b < \rho' < c$. Suppose the transformation function between the two spaces is $\rho = f(\rho', \phi'),\ \phi = \phi',\ z = z'$. The transformation function f in Fig. 2(b) should be properly chosen so

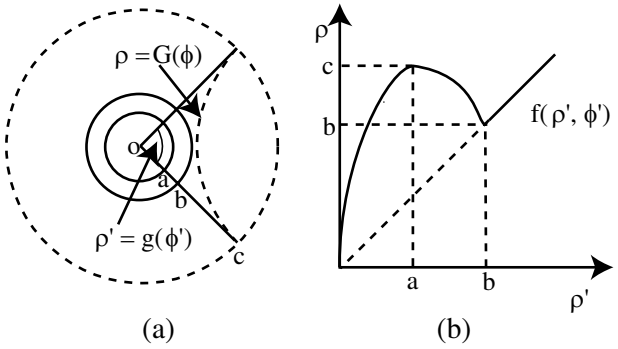

Figure 1. (a) The sketch map of transformation. (b) The transformation function $\rho = f(\rho', \phi')$.

that the function $\rho = G(\phi)$ represents a parabola.

Certainly, when the small arbitrary reflector indicated by the function $\rho' = g(\phi')$ is located in the region $a < \rho' < b$, we also achieve the same effect by changing the transformation function $\rho = f(\rho', \phi')$ in the region $a < \rho' < b$. Based on the above transformations, we can get relative permittivity and permeability tensors in the transformed space. It means that we can make an arbitrary PEC slab behave like a bigger parabola reflector.

In order to demonstrate the effectiveness of the transformation method, two examples are carried out and shown bellow.

3. ANTENNA CREATED WITH LINEAR TRANSFORMATIONS

In the cylindrical coordinate system, when $\rho' = g(\phi')$ represents a parabola, the small reflector is a parabolic antenna. Assume the coordinate transformation between the original space (ρ, ϕ, z), and the new transformed space (ρ', ϕ', z') is

$$\rho = f(\rho'),\ \phi = \phi',\ z = z' \tag{1}$$

The coordinate transformation demonstrated by Eq. (1) represents a change of the free space in the original space to a spatially varying anisotropic medium in the transformed space. Maxwell's equations are invariant under space transformation. The associated relative permittivity and permeability tensors in the transformed space as a

result of the coordinate transformation are

$$\begin{aligned}\bar{\bar{\varepsilon}}' &= \mathrm{diag}(\varepsilon_p, \varepsilon_\phi, \varepsilon_z) \\ &= \mathrm{diag}\left(\frac{f(\rho')}{\rho'}, f'(\rho'), \frac{f(\rho')f'(\rho')}{\rho'}\right) \cdot \bar{\bar{\varepsilon}} \cdot \mathrm{diag}\left(\frac{1}{f'(\rho')}, \frac{\rho'}{f(\rho')}, 1\right) \\ \bar{\bar{\mu}}' &= \mathrm{diag}(\mu_p, \mu_\phi, \mu_z) \\ &= \mathrm{diag}\left(\frac{f(\rho')}{\rho'}, f'(\rho'), \frac{f(\rho')f'(\rho')}{\rho'}\right) \cdot \bar{\bar{\mu}} \cdot \mathrm{diag}\left(\frac{1}{f'(\rho')}, \frac{\rho'}{f(\rho')}, 1\right)\end{aligned} \tag{2}$$

In this example, for simplicity, linear transformation function is used and is shown as follows, which denotes that the c/a is the amplification coefficient.

$$\rho = f(\rho') = \begin{cases} \frac{c}{a}\rho', & (\rho' < a) \\ \frac{b^2}{\rho'}\rho', & (a \le \rho' \le b) \\ \rho', & (\rho' > b) \end{cases}, \tag{3}$$

which is demonstrated by Fig. 2. We set $a = 2$, $b = 4$ and $c = 8$ which denotes that the amplification coefficient is 4, very simple parameters can be got using this transformation function [19], and the relative permittivity and permeability tensors of the transformation media are obtained as

$$\begin{cases} \mu'_\rho = 1 \ \varepsilon'_\rho = 1 \\ \mu'_\phi = 1 \ \varepsilon'_\phi = 1 \\ \mu'_z = 16 \ \varepsilon'_z = 16 \end{cases} \quad (0 \le \rho' \le 2)$$

$$\begin{cases} \mu'_\rho = -1 \ \varepsilon'_\rho = -1 \\ \mu'_\phi = -1 \ \varepsilon'_\phi = -1 \\ \mu'_z = -256/\rho'^4 \ \varepsilon'_z = -256/\rho'^4 \end{cases} \quad (2 < \rho' \le 4) \tag{4}$$

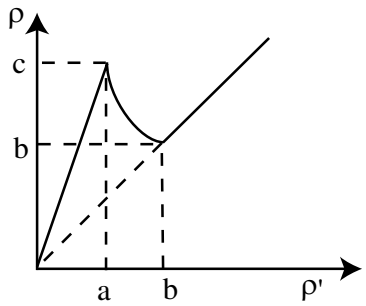

Figure 2. The linear function $\rho = f(\rho')$ for the coordinate transformation.

Here, we can see that dense material is now filled in the center region. The center region is surrounded by a cylindrical shell with negative index materials (NIM). Using the above parameters, the proposed antenna can be fabricated by properly designed metamaterials. Here, we carried out FEM based numerical simulations to verify the behavior of this type of antenna directly using the proposed parameters.

We give the simulation result based on the FEM as shown by Fig. 3(a). A small parabola antenna is put in the region surrounded by NIM shell, and the source is put on the focal point of the effective parabola outside the shell. From the simulation results, we can see that the waves come out from the shell, and most of which propagate with a flat phase front to the far-field region.

For comparison, the simulation of a parabola antenna, which is counterpart in its original space, is also carried out, as shown by Fig. 3(b). The large parabola antenna has a diameter of 4 times larger than the small parabola antenna, and the source is put on its focal point. The electric field distribution is shown in Fig. 3(b). From the two simulation results, we can see that the field distributions in the right region are very similar, which indicates the effectiveness of this type of design method. However, the electric field distributions of the two results are a little different in the some regions due to the memory restriction of the computer in the simulation. The simulation results of the proposed antenna can be the same as the original large antenna if the mesh can be infinitely small.

Finally, we put the source in the region inside the NIM shell, on

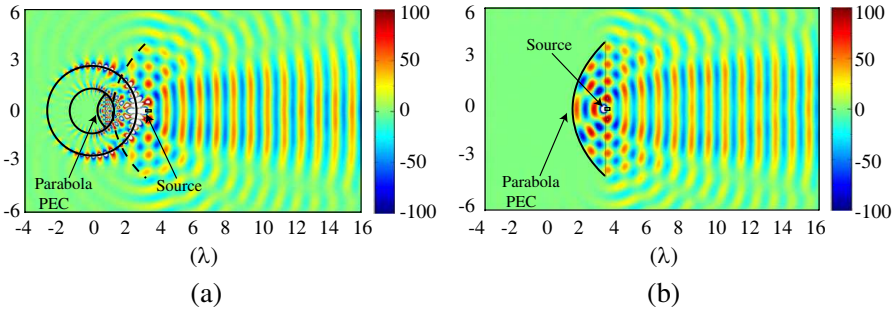

Figure 3. Snapshot of the electric field distributions of the two antennas. (a) The electric field distributions induced by a smaller the parabola antenna (the aperture is 6) in the NIM cylindrical shell, where the black dashed line demonstrates the large effective parabolic antenna. (b) The electric field distributions induced by the large the parabola antenna in the original space.

the focal point of the small parabola reflector. The field distribution is shown in Fig. 4(a), which is very similar to the results as shown in Fig. 4(b). In order to verify the results further, we give the curves of gain of the two antennas. In Fig. 4(c), we find that the gains are nearly the same. The largest gain of the large parabola reflector is 29.3 dB, and the largest gain of the small reflector is 28.6 dB. That is to say, this type of antenna can work well whether the source is putted inside or outside of the NIM shell, which will be an advantage in practical applications.

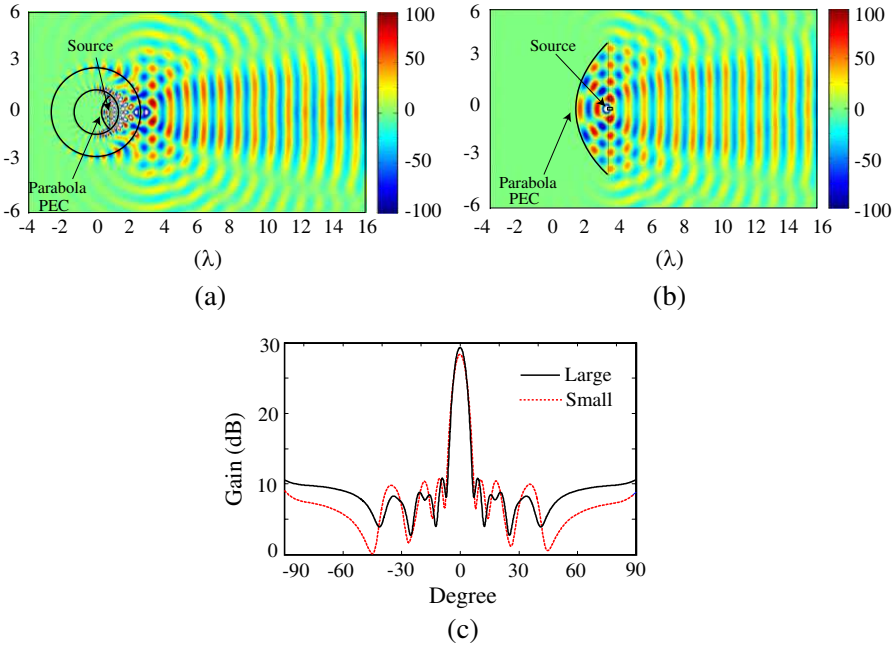

Figure 4. (a) Snapshot of the total electric field when the source is located in the center region surrounded by a NIM shell. (b) Snapshot of the total electric field of the effective large parabola reflector. (c) The gains of the two reflectors: the "Large" denotes the gain of large parabola reflector in (b), and the "Small" denotes the gain of small parabola reflector in (a).

4. ANTENNA CREATED WITH NONLINEAR TRANSFORMATIONS

In the previous part, the linear transformation can realize large effective aperture antenna which needs two kinds of anisotropic materials with complex parameters. And the fabrication of parabolic antenna is not easy, so we expect to find another transformation which can simplify the parameters. We consider the case when $\rho' = \mathrm{g}(\phi')$ represents a semicircular line, as shown by Fig. 5(a). In most of the cases, the transformation functions are dependent on ϕ, in order to create a large effective the parabola antenna from a semicircular reflector, which will result in complex parameters. In order to get simple parameters for the transformation media, the transformation function should be properly chosen so that it is independent of ϕ. In this example, the transformation function is shown as

$$\begin{aligned} \rho = f(\rho') &= \begin{cases} 4\rho' & (0 \le \rho' \le \sqrt{2}) \\ \frac{8(\rho' - \sqrt{2\rho'^2 - 4})}{(4 - \rho'^2)}, & (\sqrt{2} < \rho' \le 2) \\ \rho', & (\rho' > 2) \end{cases} \\ \phi &= \phi' \\ z &= z' \end{aligned} \tag{5}$$

And the function $f(\rho')$ is shown as in Fig. 5(b). This nonlinear transformation compresses the original space in the center region of the transformed space, and the parabola $\rho' = g(\phi')$ becomes $\rho = G(\phi)$.

The corresponding relative permittivity and permeability tensors of the material in the cylindrical shell in cylindrical coordinate can be

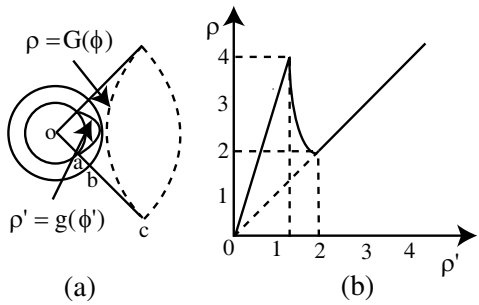

Figure 5. (a) The transformation scheme. (b) The transformation function.

derived as

$$\begin{cases} \varepsilon'_\rho = \mu'_\rho = 1 \\ \varepsilon'_\phi = \mu'_\phi = 1 \qquad (0 \le \rho' \le \sqrt{2}) \\ \varepsilon'_z = \mu'_z = 16 \end{cases}$$

$$\begin{cases} \varepsilon'_\rho = \mu'_\rho = \dfrac{\left(\rho' - \sqrt{2\rho'^2 - 4}\right)\left(4 - \rho'^2\right)}{\rho'\left(\left(1 - \frac{2\rho'}{\sqrt{2\rho'^2-4}}\right)\left(4-\rho'^2\right) + 2\rho'\left(\rho' - \sqrt{2\rho'^2-4}\right)\right)} \\ \varepsilon'_\phi = \mu'_\phi = \dfrac{\rho'\left(\left(1 - \frac{2\rho'}{\sqrt{2\rho'^2-4}}\right)\left(4-\rho'^2\right) + 2\rho'\left(\rho' - \sqrt{2\rho'^2-4}\right)\right)}{\left(\rho' - \sqrt{2\rho'^2-4}\right)\left(4-\rho'^2\right)} \qquad (\sqrt{2} < \rho' \le 2) \\ \varepsilon'_z = \mu'_z = \\ \dfrac{64\left(\rho' - \sqrt{2\rho'^2-4}\right)\left(\left(1 - \frac{2\rho'}{\sqrt{2\rho'^2-4}}\right)\left(4-\rho'^2\right) + 2\rho'\left(\rho' - \sqrt{2\rho'^2-4}\right)\right)}{\rho'\left(4-\rho'^2\right)^3} \end{cases} \tag{6}$$

The simulations can be carried out by using the parameters in formula (6). Fig. 6(a) shows the electric distributions of the designed antenna. Similar to Fig. 3, the small semicircular reflector is put in the center region and surrounded by a NIM shell. The source in the transformed space is put on the effective focal point of the original parabola in the original space. Fig. 6(b) shows the electric field distributions of the large parabolic antenna in the original space. Here, the aperture of the proposed antenna is 4 times of the small semicircular reflector. If we want to get larger effective apertures, the

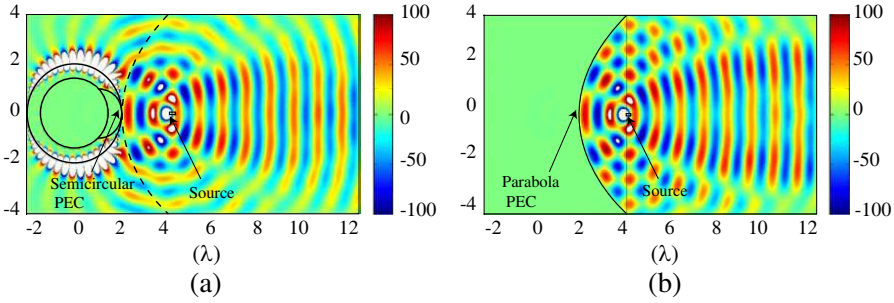

Figure 6. Snapshot of the electric field distributions of the two antennas. (a) The electric field distributions induced by a smaller semicircular PEC reflector in the NIM cylindrical shell, where the black dashed line demonstrates the large effective parabola antenna. (b) The electric field distributions induced by the large parabolic antenna in the original space (the aperture is 4 times larger than the small semicircular PEC reflector).

transformation functions can also be easily determined. Using this transformation, we can get a large parabolic antenna by surrounding a semicircular metal construction with a NIM shell.

5. CONCLUSION

A new method for designing small size antenna with large effective apertures is presented in this paper. Using the multi-valued transformation function, the large original space is compressed into a small center region in the transformed space and surrounded by a NIM shell resulted from the negative slope of the transformation function. This type of coordinate transformation is then able to amplify the aperture of the small reflectors. Two examples using linear and nonlinear transformation functions are shown to demonstrate the effectiveness of this method. Our current results are carried out in the two dimensional cases. However, this method can also be easily extended to the three dimensional cases.

ACKNOWLEDGMENT

This work is sponsored by the ZJNSF (No. Y1080715), 863 Project (No. 2009AA01Z227), NSFC (No. 60531020, 60701007), NCET-07-0750 and the National Key Laboratory Foundation (No. 9140C5304020901), ZJSTP (No. 2009C31141).

REFERENCES

1. Pendry, J. B., D. Schurig, and D. R. Smith, "Controlling electromagnetic fields," *Science*, Vol. 312, 1780–1782, 2006.
2. Leonhardt, U. and T. G. Philbin, "General relativity in electrical engineering," *New J. Phys.*, Vol. 8, 247, 2006.
3. Schurig, D., J. J. Mock, B. J. Justice, S. A. Cummer, J. B. Pendry, A. F. Starr, and D. R. Smith, "Metamaterial electromagnetic cloak at microwave frequencies," *Science*, Vol. 314, 977–980, 2006.
4. Cummer, S. A., B.-I. Popa, D. Schurig, D. R. Smith, and J. Pendry, "Full-wave simulations of electromagnetic cloaking structures," *Phys. Rev. E*, Vol. 74, 036621–036625, 2006.
5. Chen, H. S., B. I. Wu, B. Zhang, and J. A. Kong, "Electromagnetic wave interactions with a metamaterial cloak," *Phys. Rev. Lett.*, Vol. 99, 063903–063906, 2007.
6. Zhang, B., H. S. Chen, B. I. Wu, Y. Luo, L. X. Ran, and J. A. Kong, "Response of a cylindrical invisibility cloak to

electromagnetic waves," *Physical Review B*, Vol. 76, 121101–121105, 2007.

7. Zhang, J. J., J. T. Huangfu, Y. Luo, H. S. Chen, J. A. Kong, and B. I. Wu, "Cloak for multilayered and gradually changing media," *Physical Review B*, Vol. 77, 035116–035120, 2008.
8. Han, T. C., X. H. Tang, and F. Xiao, "The petal-shaped cloak," *Journal of Electromagnetic Waves and Applications*, Vol. 23, No. 14–15, 2055–2062, 2009.
9. Zhang, B., H. Chen, and B.-I. Wu, "Practical limitations of an invisibility cloak," *Progress In Electromagnetics Research*, Vol. 97, 407–416, 2009.
10. Cheng, Q., W. X. Jiang, and T.-J. Cui, "Investigations of the electromagnetic properties of three-dimensional arbitrarily-shaped cloaks," *Progress In Electromagnetics Research*, Vol. 94, 105–117, 2009.
11. Cheng, X., H. Chen, B.-I. Wu, and J. A. Kong, "Cloak for bianisotropic and moving media," *Progress In Electromagnetics Research*, Vol. 89, 199–212, 2009.
12. Cheng, X., H. Chen, X.-M. Zhang, B. Zhang, and B.-I. Wu, "Cloaking a perfectly conducting sphere with rotationally uniaxial nihility media in monostatic radar system," *Progress In Electromagnetics Research*, Vol. 100, 285–298, 2010.
13. Xi, S., H. S. Chen, B. I. Wu, and J. A. Kong, "One-directional perfect cloak created with homogeneous material," *IEEE Microwave and Wireless Components Letters*, Vol. 19, 131–133, 2009.
14. Greenleaf, A., M. Lassas, and G. Uhlmann, "Anisotropic conductivities that cannot be detected by EIT," *Physiol. Meas.*, Vol. 24, 413–416, 2003.
15. Zhang, J. J., Y. Luo, S. Xi, H. S. Chen, L. X. Ran, B. I. Wu, and J. A. Kong, "Directive emission obtained by coordinate transformation," *Progress In Electromagnetics Research*, Vol. 81, 437–446, 2008.
16. Pu, T. L., K. M. Huang, B. Wang, and Y. Yang, "Application of micro-genetic algorithm to the design of matched high gain patch antenna with zero-refractive-index metamaterial lens," *Journal of Electromagnetic Waves and Applications*, Vol. 24, No. 8-9, 1207–1217, 2010.
17. Zhang, J. J., Y. Luo, H. Chen, and B.-I. Wu, "Sensitivity of transformation cloak in engineering," *Progress In Electromagnetics Research*, Vol. 84, 93–104, 2008.

18. Yu, G. X., T. J. Cui, W. X. Jiang, X. M. Yang, Q. Cheng, and Y. Hao, "Transformation of different kinds of electromagnetic waves using metamaterials," *Journal of Electromagnetic Waves and Applications*, Vol. 23, No. 5–6, 583–592, 2009.
19. Donderici, B. and F. L. Teixeira, "Metamaterial blueprints for reflectionless waveguide bends," *IEEE Microwave and Wireless Components Letters*, Vol. 18, 233–235, 2008.
20. Alu, A. and N. Engheta, "Achieving transparency with plasmonic and metamaterial coatings," *Phys. Rev. E*, Vol. 72, 016623–016631, 2005.
21. Leonhardt, U., "Optical conformal mapping," *Science*, Vol. 312, 1777–1780, 2006.
22. Popa, B.-I. and S. A. Cummer, "Cloaking with optimized homogeneous anisotropic layers," *Physical Review A*, Vol. 79, 023806–023804, 2009.
23. Pendry, J. B., "Perfect cylindrical lenses," *Opt. Express*, Vol. 11, 755–760, 2003.
24. Luo, Y., H. Chen, J. Zhang, L. Ran, and J. A. Kong, "Design and analytical full-wave validation of the invisibility cloaks, concentrators, and field rotators created with a general class of transformations," *Physical Review B*, Vol. 77, 125127–125128, 2008.
25. Yan, M., W. Yan, and M. Qiu, "Cylindrical superlens by a coordinate transformation," *Physical Review B*, Vol. 78, 125113–125117, 2008.
26. Yang, T., H. Chen, X. Luo, and H. Ma, "Superscatterer: Enhancement of scattering with complementary media," *Opt. Express*, Vol. 16, 18545–18550, 2008.
27. Yu, G. X., T. J. Cui, W. X. Jiang, X. M. Yang, Q. Cheng, and Y. Hao, "Transformation of different kinds of electromagnetic waves using metamaterials," *Journal of Electromagnetic Waves and Applications*, Vol. 23, No. 5–6, 583–592, 2009.
28. Ferrara, F., C. Gennarelli, R. Guerriero, G. Riccio, and C. Savarese, "An efficient near-field to far-field transformation using the planar wide-mesh scanning," *Journal of Electromagnetic Waves and Applications*, Vol. 21, No. 3, 341–357, 2007.
29. Erentok, A. and R. W. Ziolkowski, "Metamaterial-inspired efficient electrically small antennas," *IEEE Trans. Antennas Propag.*, Vol. 56, 691–707, 2008.
30. Hwang, R.-B., H.-W. Liu, and C.-Y. Chin, "A metamaterial-based E-plane horn antenna," *Progress In Electromagnetics Research*,

Vol. 93, 275–289, 2009.

31. Jarchi, S., J. Rashed-Mohassel, and R. Faraji-Dana, "Analysis of microstrip dipole antennas on a layered metamaterial substrate," *Journal of Electromagnetic Waves and Applications*, Vol. 24, No. 5–6, 755–764, 2010.
32. Zhou, H., S. Qu, Z. Pei, Y. Yang, J. Zhang, J. Wang, H. Ma, C. Gu, X. Wang, Z. Xu, W. Peng, and P. Bai, "A High-directive patch antenna based on all-dielectric near-zero-index metamaterial superstrates," *Journal of Electromagnetic Waves and Applications*, Vol. 24, No. 10, 1387–1396, 2010.
33. Hong, T., S.-X. Gong, W. Jiang, Y.-X. Xu, and X. Wang, "A novel ultra-wide band antenna with reduced radar cross section," *Progress In Electromagnetics Research*, Vol. 96, 299–308, 2009.
34. Behera, S. and K. J. Vinoy, "Microstrip square ring antenna for dual-band operation," *Progress In Electromagnetics Research*, Vol. 93, 41–56, 2009.
35. Najjar-Khatirkolaei, B. N. and A. R. Sebak, "Slot antenna on a conducting elliptic cylinder coated by nonconfocal chiral media," *Progress In Electromagnetics Research*, Vol. 93, 125–143, 2009.